Fig. 1A *Fig.1C* *Fig. 1E*

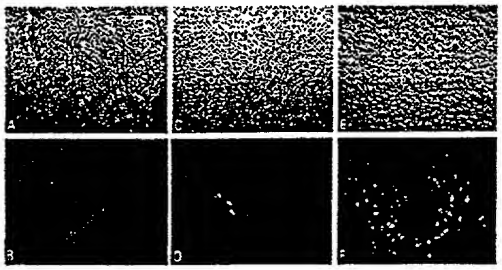

Fig. 1B *Fig. 1D* *Fig. 1F*

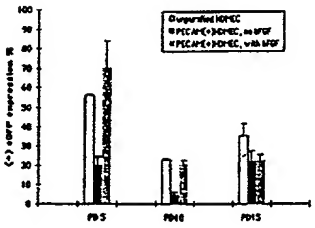

Fig. 2

Fig. 3A

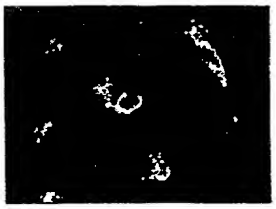

Fig. 3B

Fig. 4A

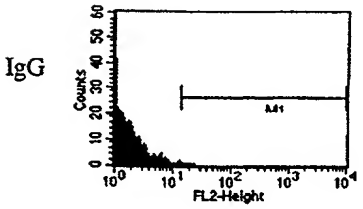

Fig. 4B

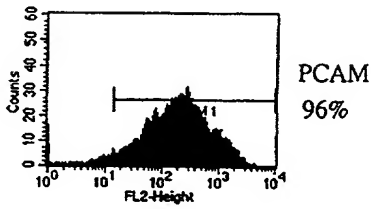

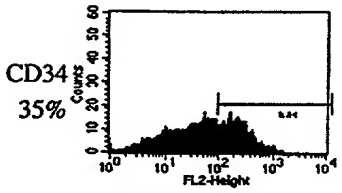

Fig. 4C

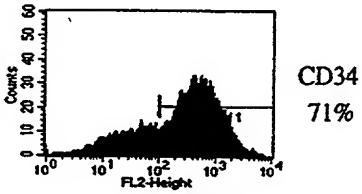

Fig. 4D

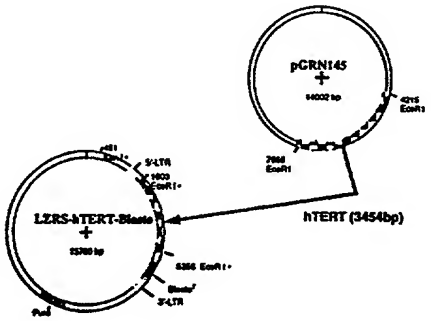

Fig. 5

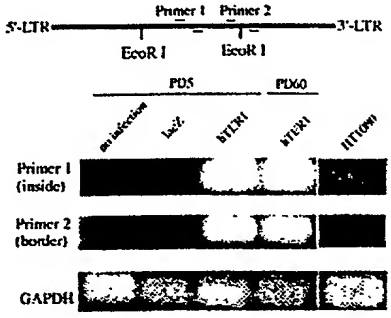
Primer 1
Primer 2
5'-LTR
3'-LTR
EcoR I
EcoR I
PD5
PD60
Primer 1 (inside)
Primer 2 (border)
GAPDH

Fig. 6

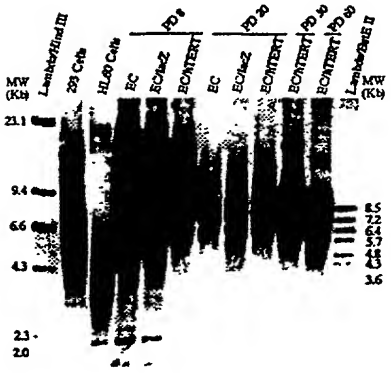
MW (Kb)
293 Cells
HL-60 Cells
EC
ECtert2
ECtert1
PD 5
PD 20
PD 30
PD 60
23.1
9.4
6.6
4.3
2.3 - 2.0
8.5
7.2
6.4
5.7
4.8
4.3
3.6

Fig. 7

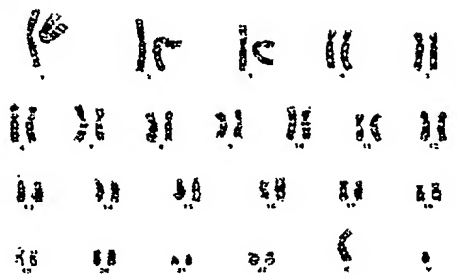

Fig.8

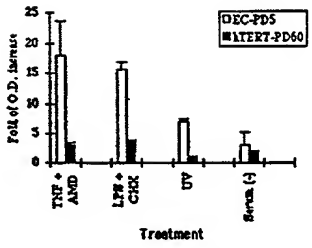

Fig. 9A

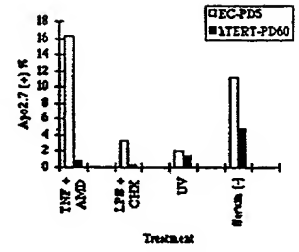

Fig. 9B

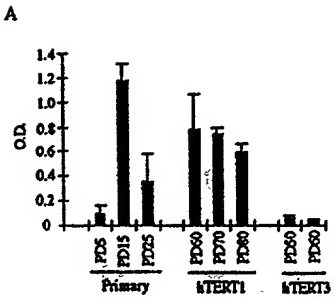

Fig. 10A

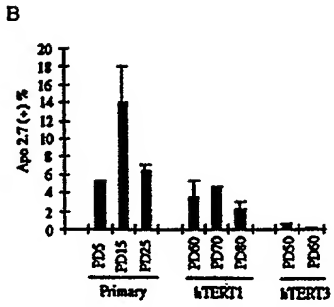

Fig. 10B

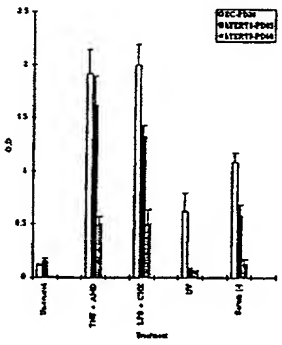

Fig. 11A

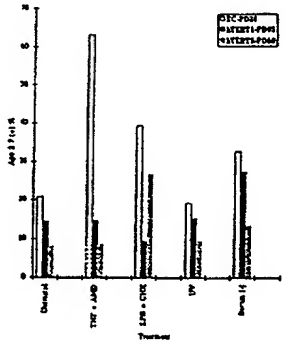

Fig. 11B

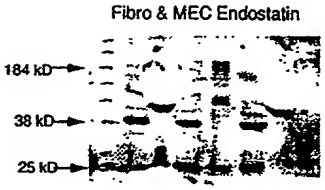

Fig. 12

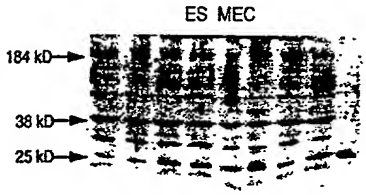

Fig. 13

Figure 14

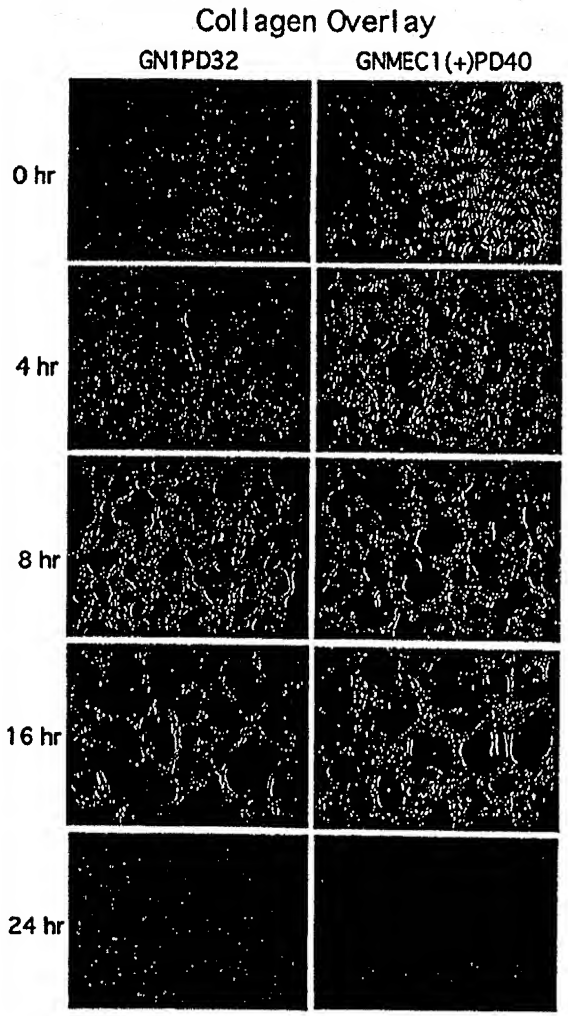

Time course of apoptotic induction by 3D collagen overlay *in vitro* and superior survival of Tert-EC versus primary parental EC. By 16hr after collagen overlay, parental cultures are undergoing dissolution and apoptosis whereas, Tert-EC are still forming tubule structures. At 24hr, all parental cells are dead and Tert-EC are stable.

GN1PD32: eGFP-labeled primary HDMEC at PD32 (mid-late passage)

GNMEC1(+)PD40: hTERT(+) GNMEC-1 at PD40

Figure 15

Time Course of High Density Matrigel Tubule Formation

4 Hr **8 Hr** **24 Hr**

Demonstration of the utility of using eGFP-labeled Tert-EC for tracking morphogenetic patterns of cells forming microvascular structures *in vitro*

Figure 16

Superiority and utility of eGFP-labeled Tert-EC in formation of vascular structures in 3D Matrigel *in vitro*.

Senescent parental EC (EC-PD38) show no vessels in 3D Matrigel compared to younger cells (EC-PD20). Vessels were numerous and prominently labeled in all Tert-EC cultures (hTERT1-PD56).

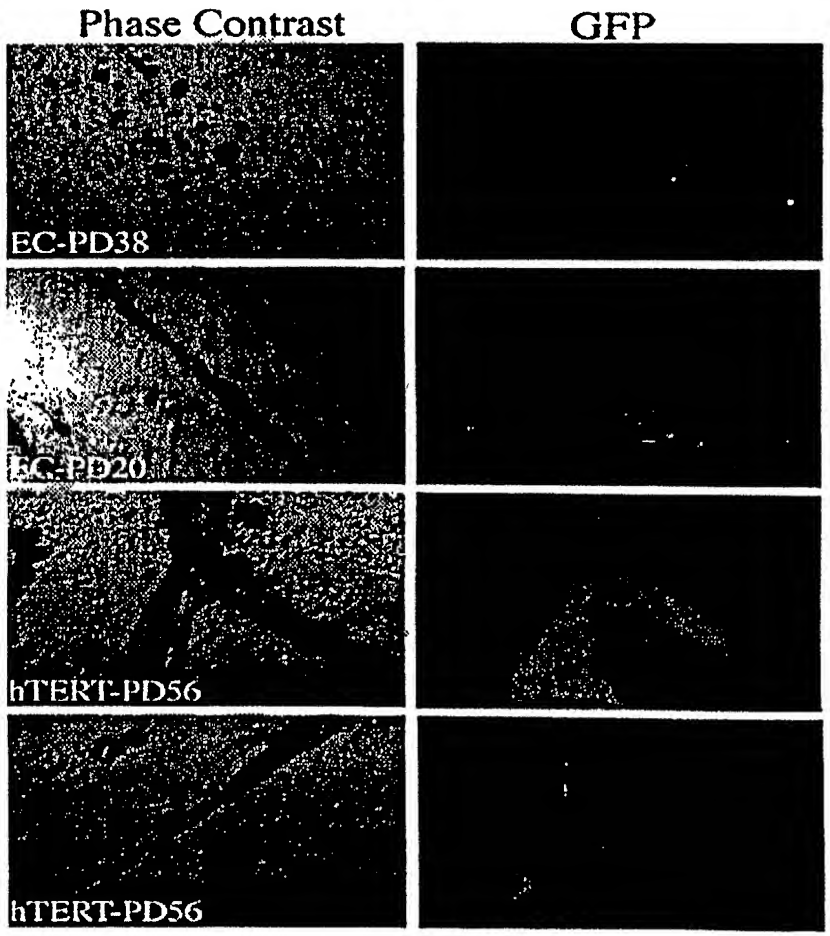

Figure 17

Inhibition of *in vitro* angiogenic web formation by cyclo-oxygenase (COX) antagonists

Tert-EC were incubated in the presence of two different COX inhibitors (indomethacin and NS-398) at different concentrations and examined 12hr after plating on Matrigel. Controls show no vessels in absence of Matrigel and numerous vessels in absence of or at low dose COX blockers. Graded inhibition of vessel formation is observed with increasing doses of COX blockers, with the COX-2 specific inhibitor (NS-398) 10-fold more potent than the general inhibitor, indomethacin.

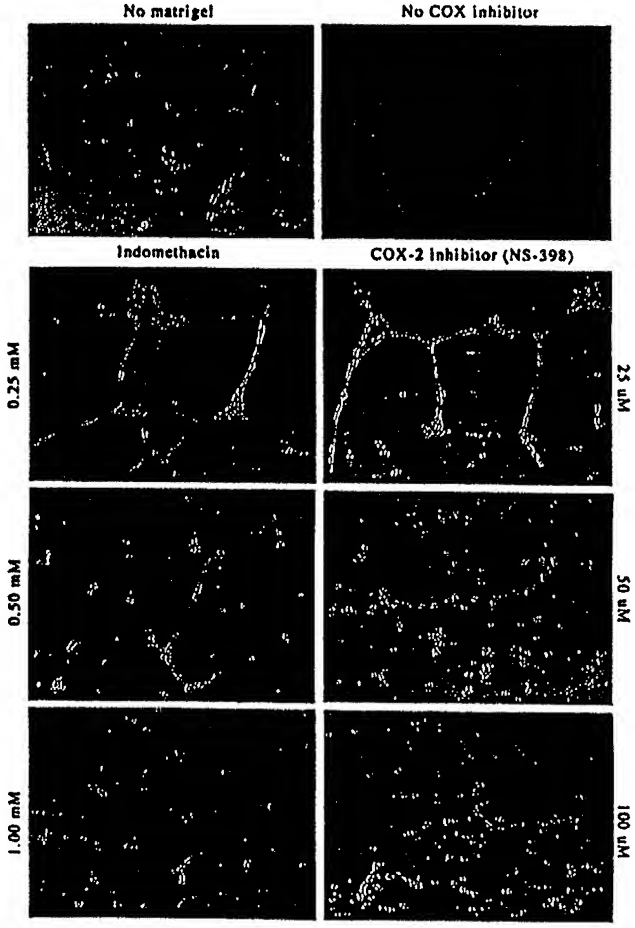

Figure 18

Tissue sections stained with H&E (A,D,G) and for anti-human Type 4 collagen (C,F,I) demonstrate the presence of host murine vessels in Matrigel implants containing bFGF (arrows) but absence of human basement membrane collagen (C). Both primary and Tert-EC demonstrate Col-4(+) vessels containing RBCs (arrows). IgG controls shows no IF reactivity (B,E,H). Results indicate human vessels have formed anastamoses with host mouse vessels (i.e. "chimeric" vessels).

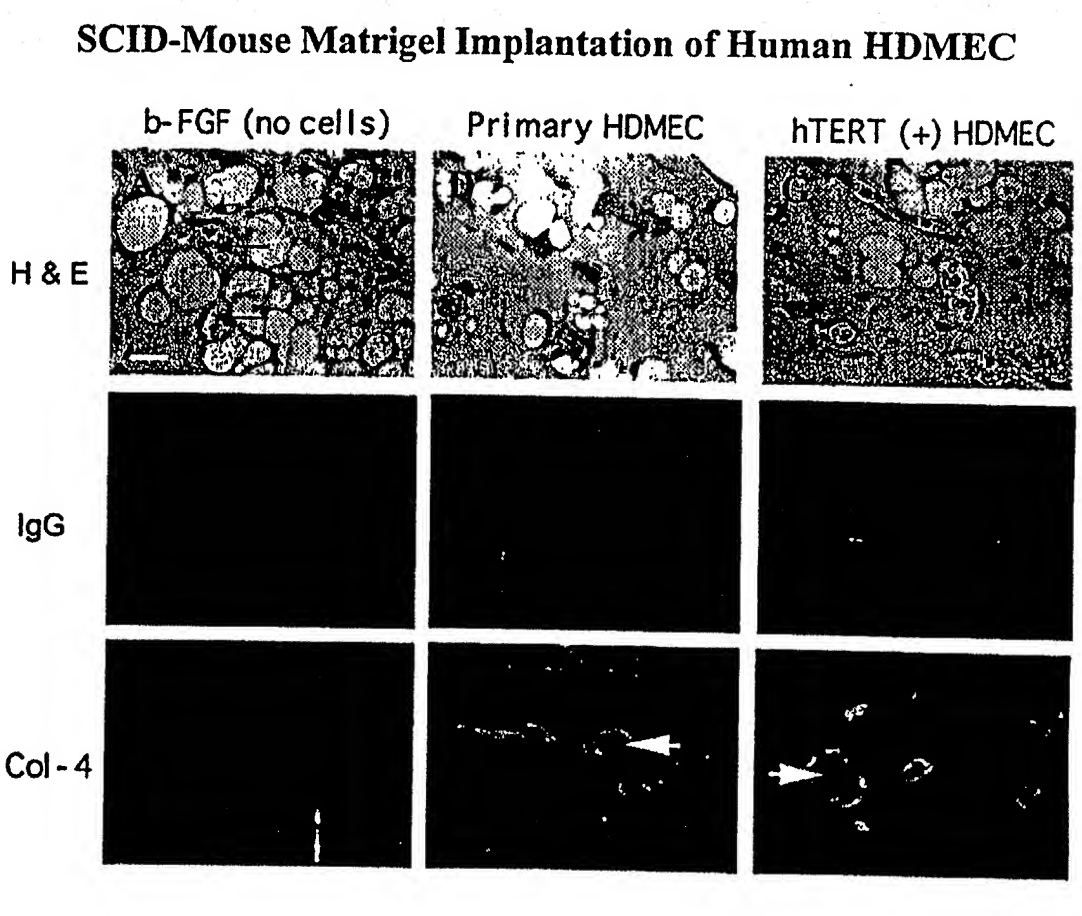

Figure 19 Superiority of Tert-EC at In Vivo Microvessel Formation

Early-mid passage parental eGFP-labeled HDMEC (GN1-PD20) were directly compared to Tert-EC line (GNMEC-1) for their ability to form fluorescent microvessels *in vivo* using the SCID mouse Matrigel implantation assay system. TertEC demonstrated more fluorescent vascular structures at all time points after implantation versus parental line.

GNMEC1 PD57

GN1 PD20

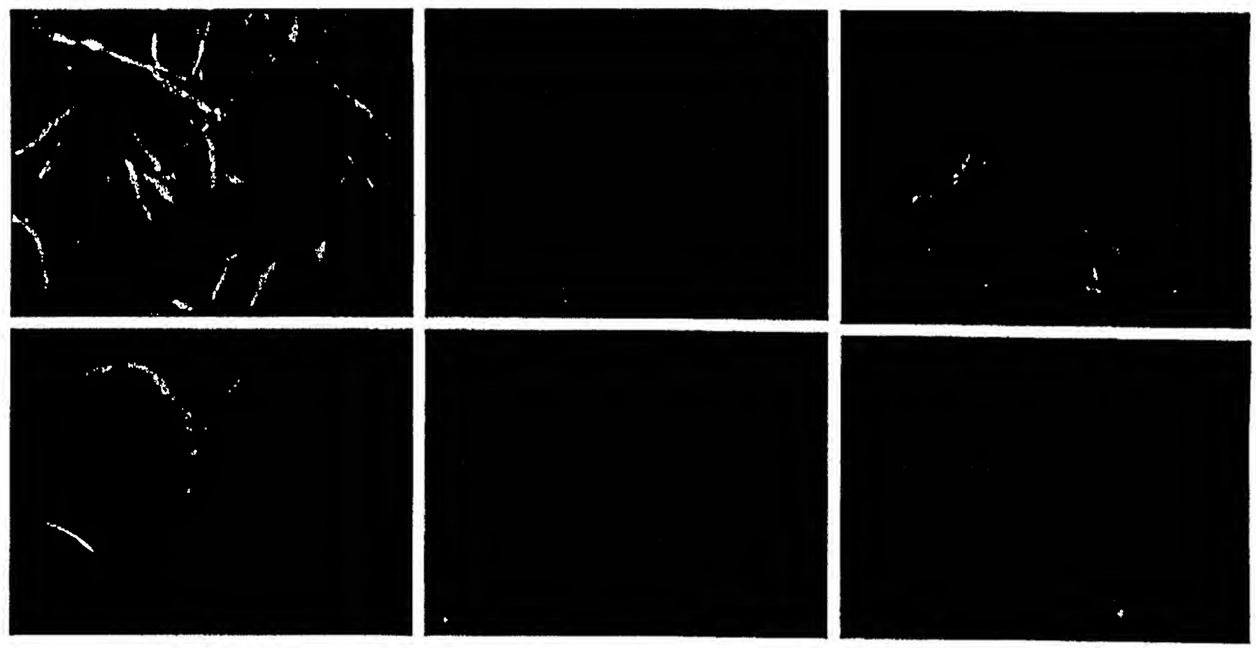

2 wk 4 wk 6 wk

Figure 20 **Superiority of Tert-EC at In Vivo Microvessel Formation**

Use of Type 4 collagen IF reactivity to quantify human microvessels *in vivo* demonstrates superior durability of Tert-EC (GNMEC1) versus late passage parental cells (GN1PD34). Younger parental cells (PD20) show many small diameter vessels.

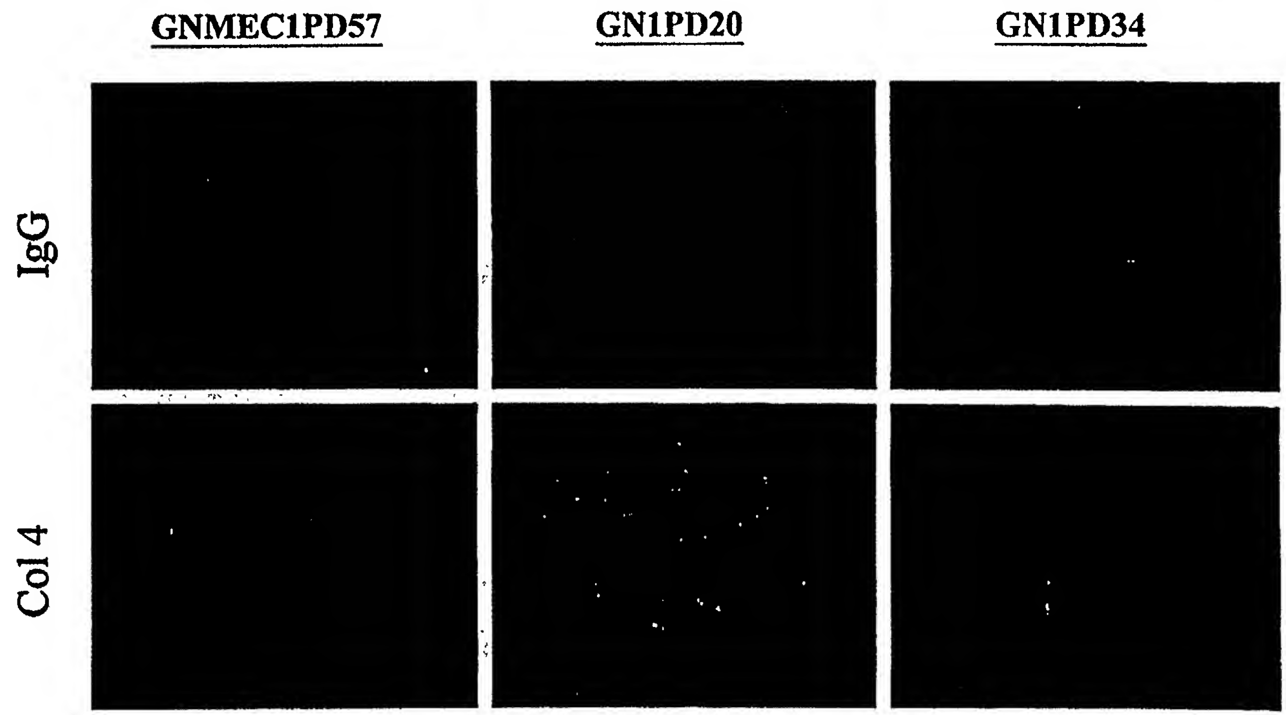

Figure 21 Superiority of Tert-EC at In Vivo Microvessel Formation

Quantitative comparison of microvessel density by IFmicromorphometry using anti-human Type 4 collagen demonstrates equal number of vessels in young primary (GN1PD12) vs Tert-EC (GNMEC1) and maintenance of vessels at 2, 4 and 6 weeks after implantation in Tert-EC (>25); whereas, mid and late passage parental EC show both decreased numbers and loss of vessels with time *in vivo*. Dermal fibroblasts (Fb) and human fibrosarcoma cells (HT-1080) show no vessel formation (see Figures 22, 23).

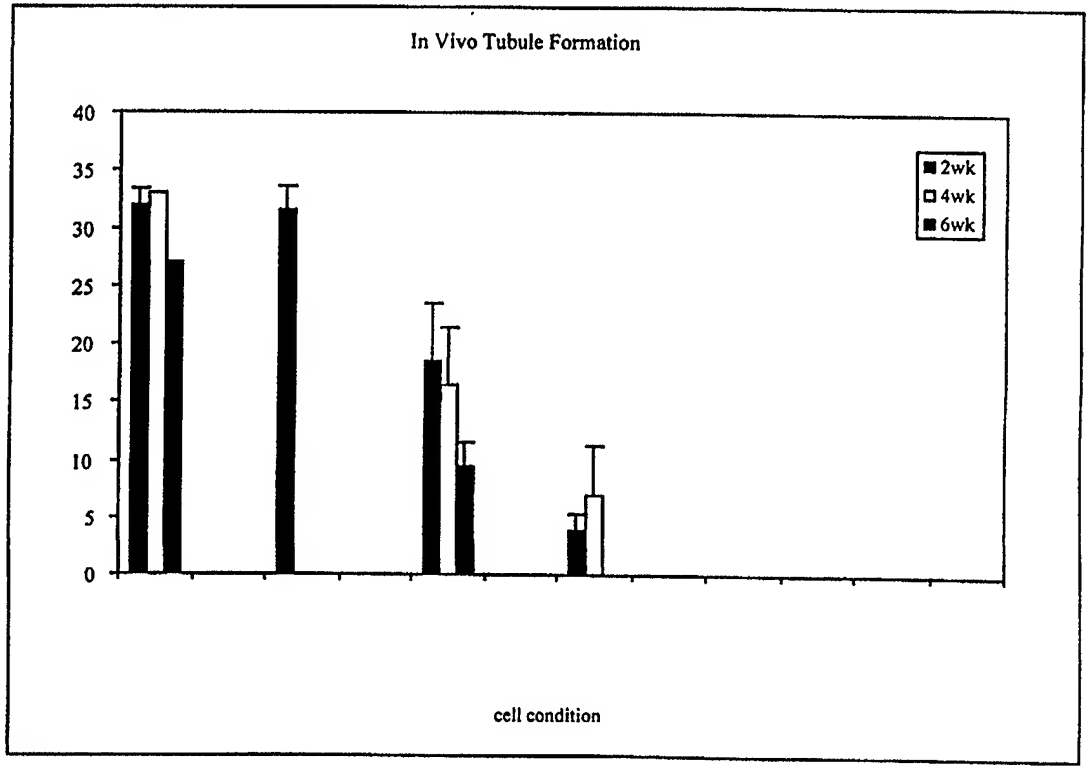

Figure 22

Specificity of Tert-EC at In Vivo Microvessel Formation

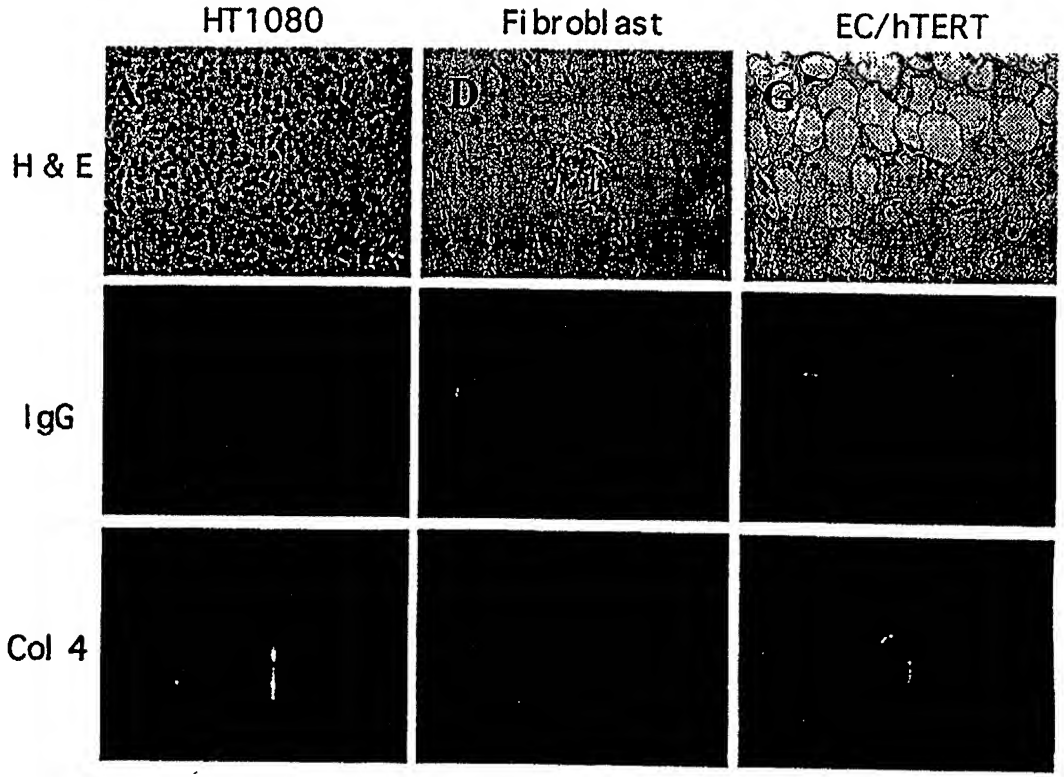

Tissue sections stained with H&E (A,D,G) and for anti-human Type 4 collagen (C,F,I) demonstrate the presence of human vessels in Matrigel implants containingTert-EC (G,I) but absence of human basement membrane collagen (C,F) in implants containing HT1080 cells or human dermal fibroblasts. IgG controls shows no IF reactivity (B,E,H). Results indicate lack of human vessel formation in implants containing nonECtypes.

Figure 23

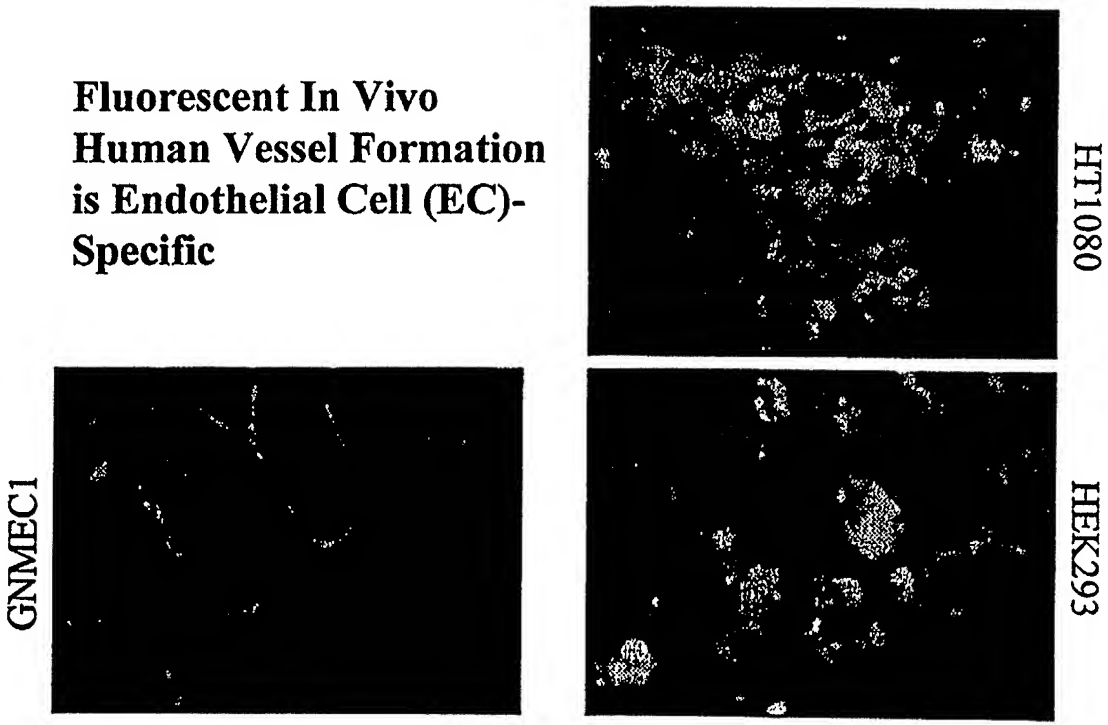

Human fibrosarcoma cells (HT1080) and human embryonic kidney tumor cells (HEK293) expressing eGFP show fluorescent tumor masses but no microvessels, whereas, Tert-EC (GNMEC1) form obvious fluorescent vessels.

Figure 24

Effect of PMA and LM609 on Vessel Formation

PMA (10 ug/ml)

LM609 (25 ug/ml)

Control

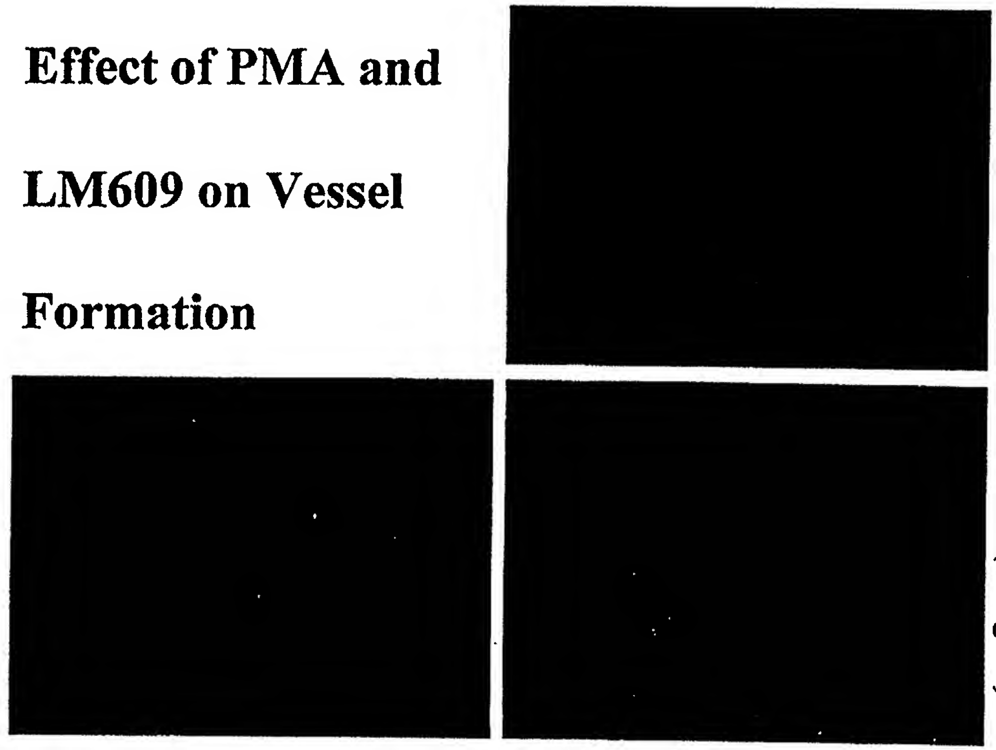

Treatment of Tert-EC with phorbol ester (PMA) or vitronectin receptor ($\alpha_V\beta_3$) -antagonist (LM609) for 2 hrs prior to implantation *in vivo*. Results show PMA has a slight negative effect on vessel density, whereas, LM609 appears to increase vessels relative to control, untreated cells.

Figure 25

Effect of PMA and LM609 on *In Vivo* Vessel Formation

Quantification of vessel density by IF staining of human Type 4 collagen shows effects of PMA and LM609, as described in Figure 24.

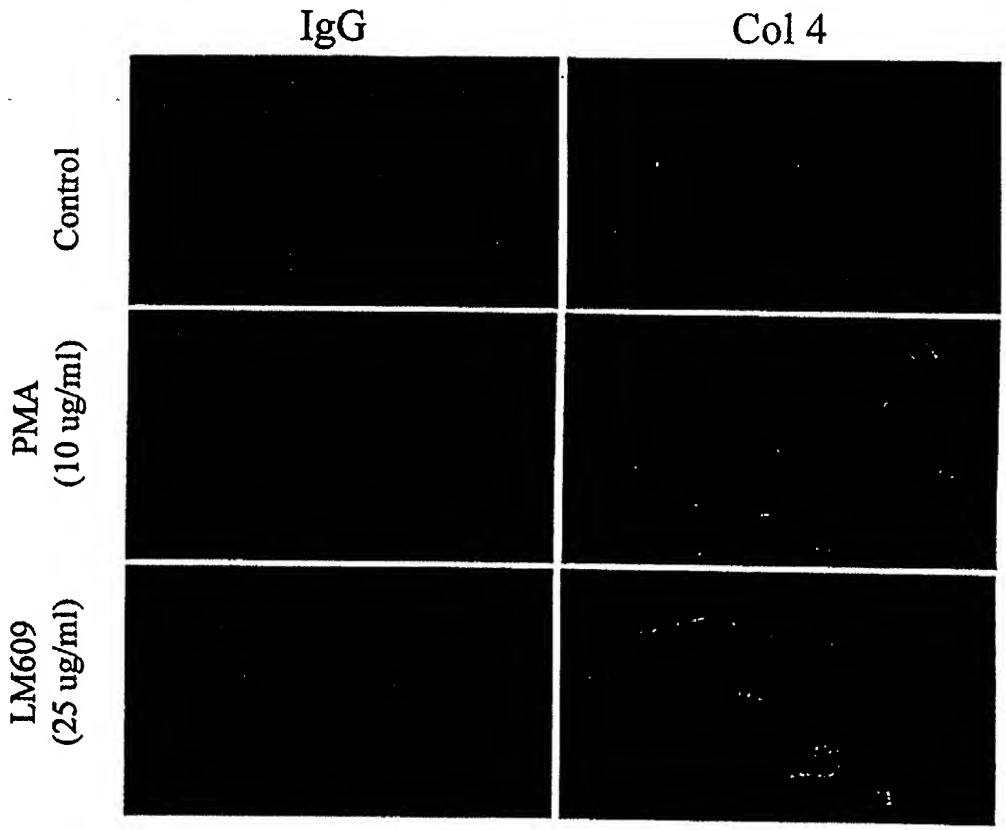

Figure 26

Quantification of vessel density by IF staining of human Type 4 collagen shows effects of b-FGF and VEGF. Results indicate FGF increases vessel density, whereas, VEGF has little effect.

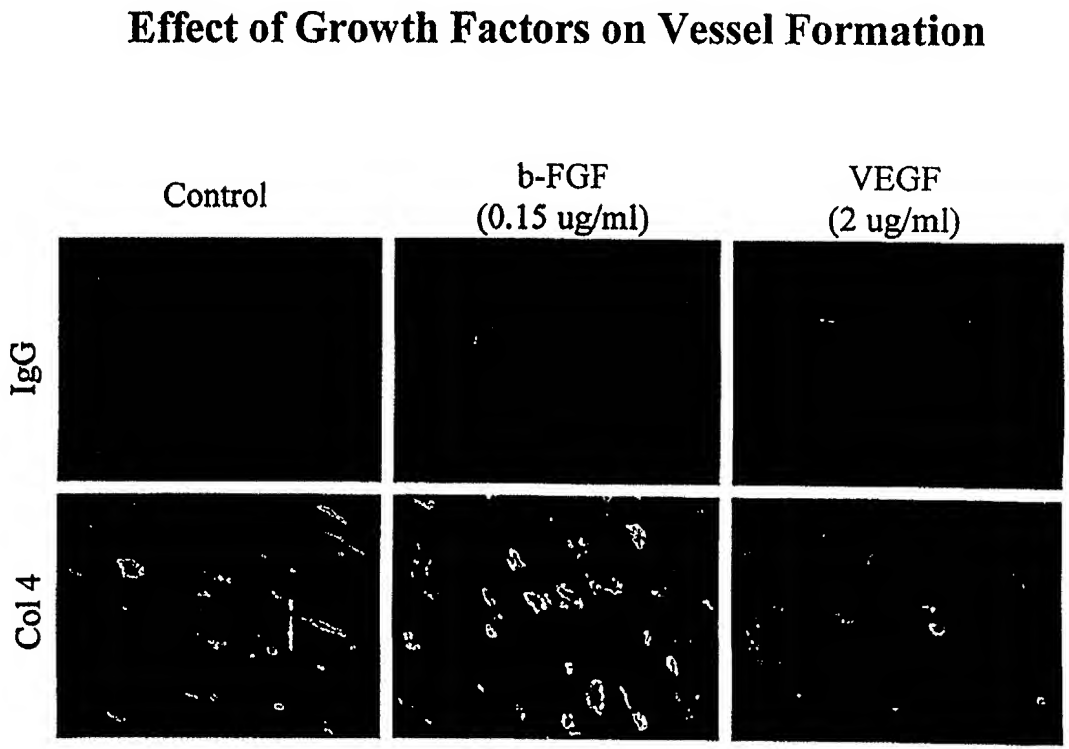

Figure 27

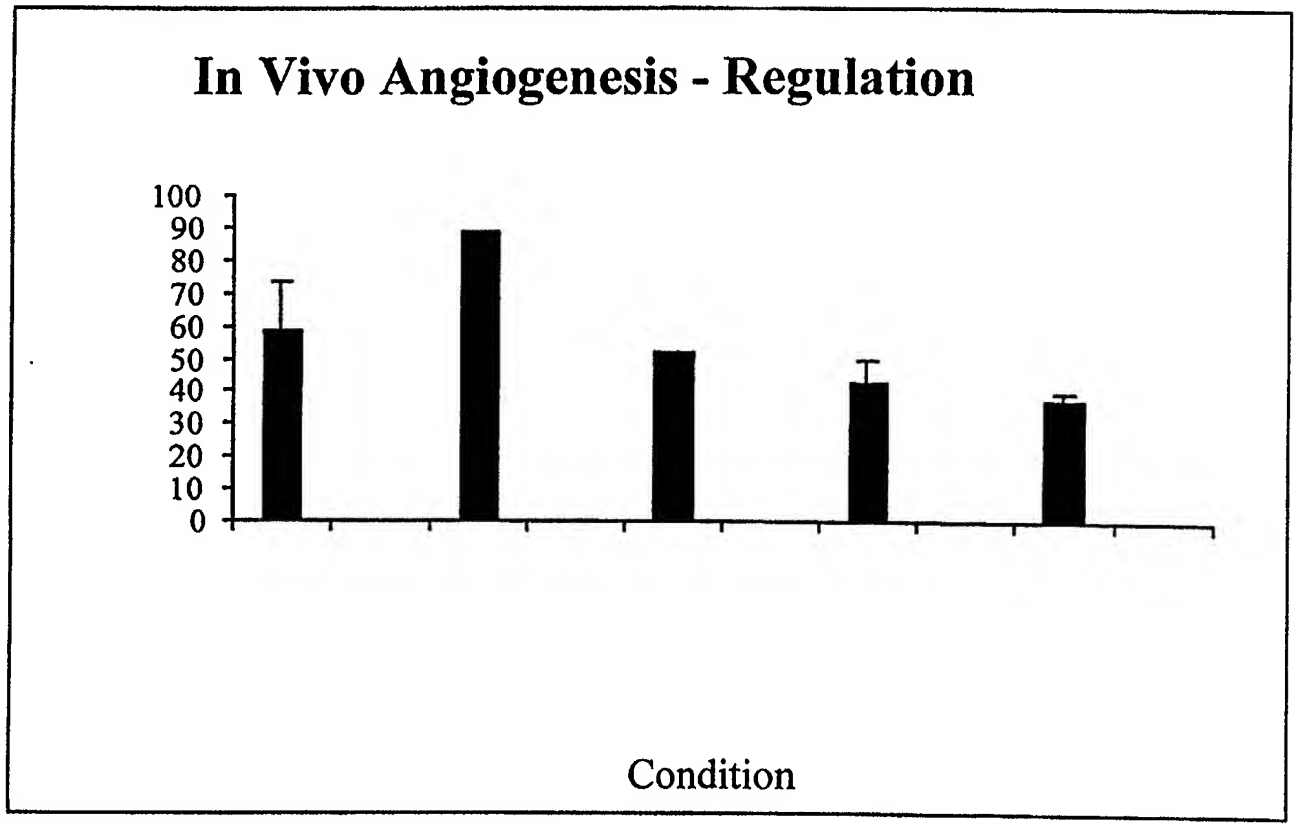

Effect of different angiogenic regulators on GNMEC1 *in vivo* microvessel formation. Results show significant changes in vessel density only by b-FGF.

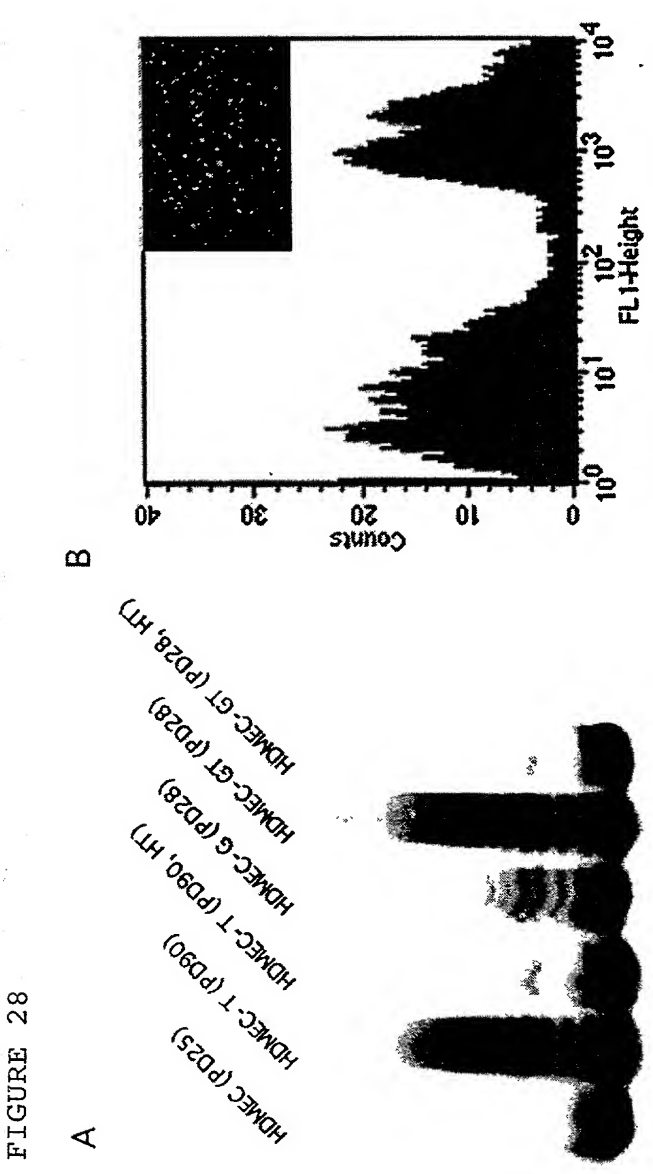

FIGURE 28

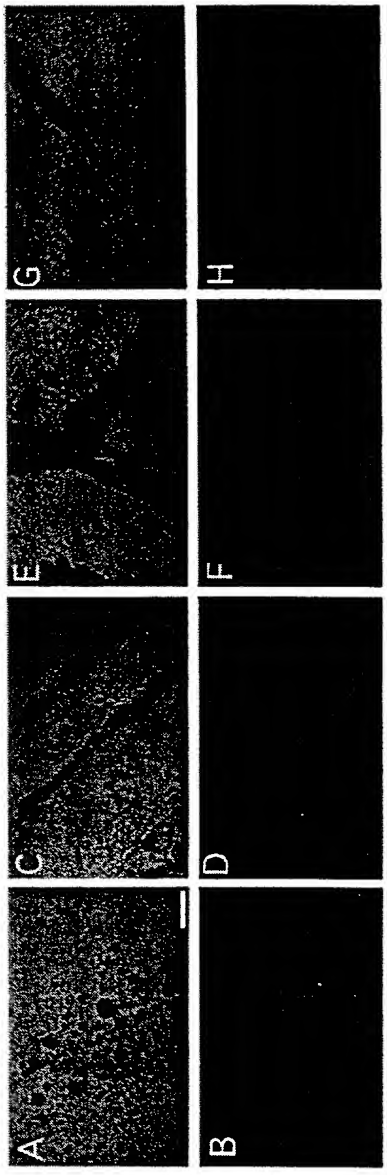

FIGURE 29

FIGURE 30

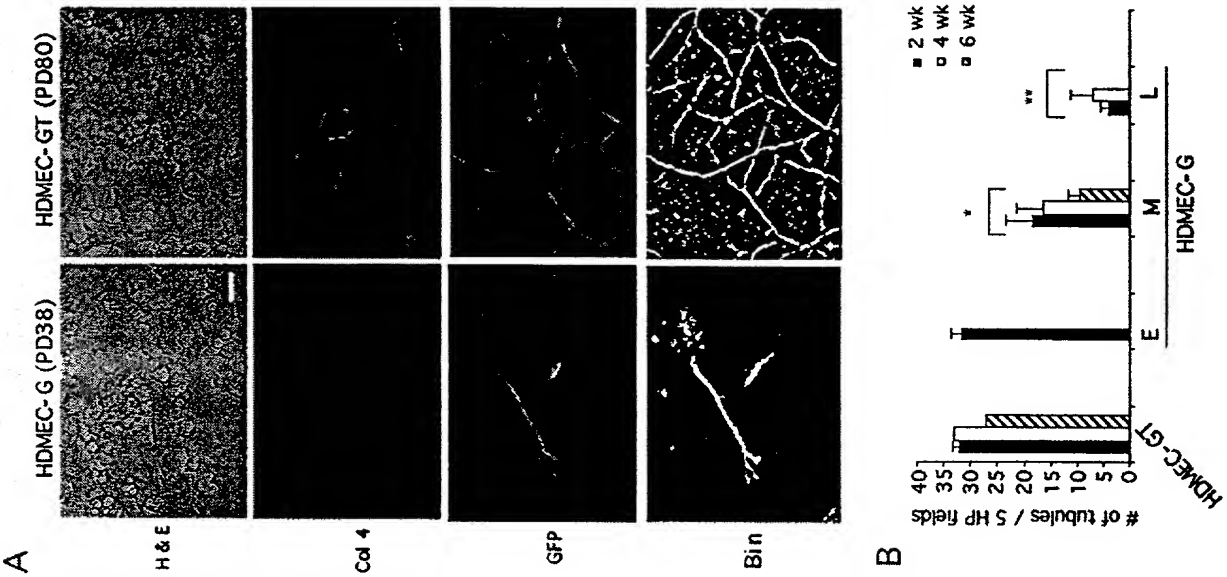
A
HDMEC-G (PD38)
HDMEC-GT (PD80)
H&E
Col 4
GFP
Bin
B
2 wk
4 wk
6 wk
# of tubules / 5 HP fields
HDMEC-GT
HDMEC-G
E
M
L
*
**

FIGURE 31

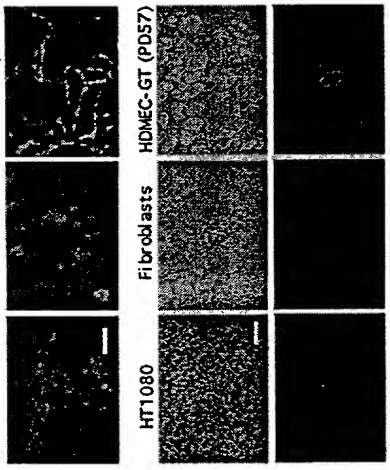

FIGURE 32

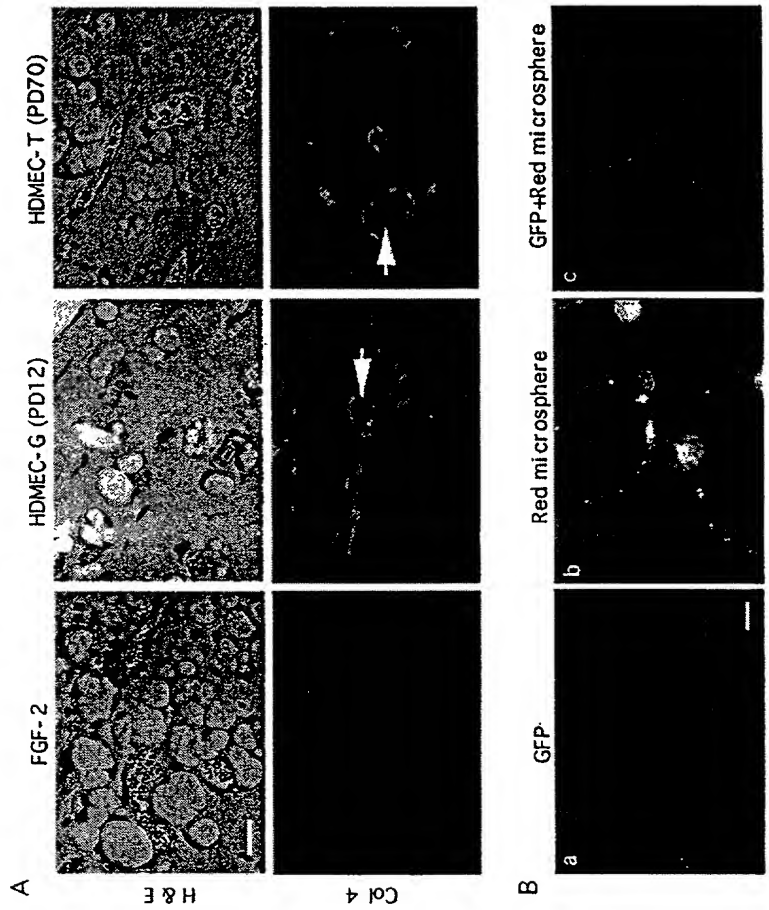

FIGURE 33

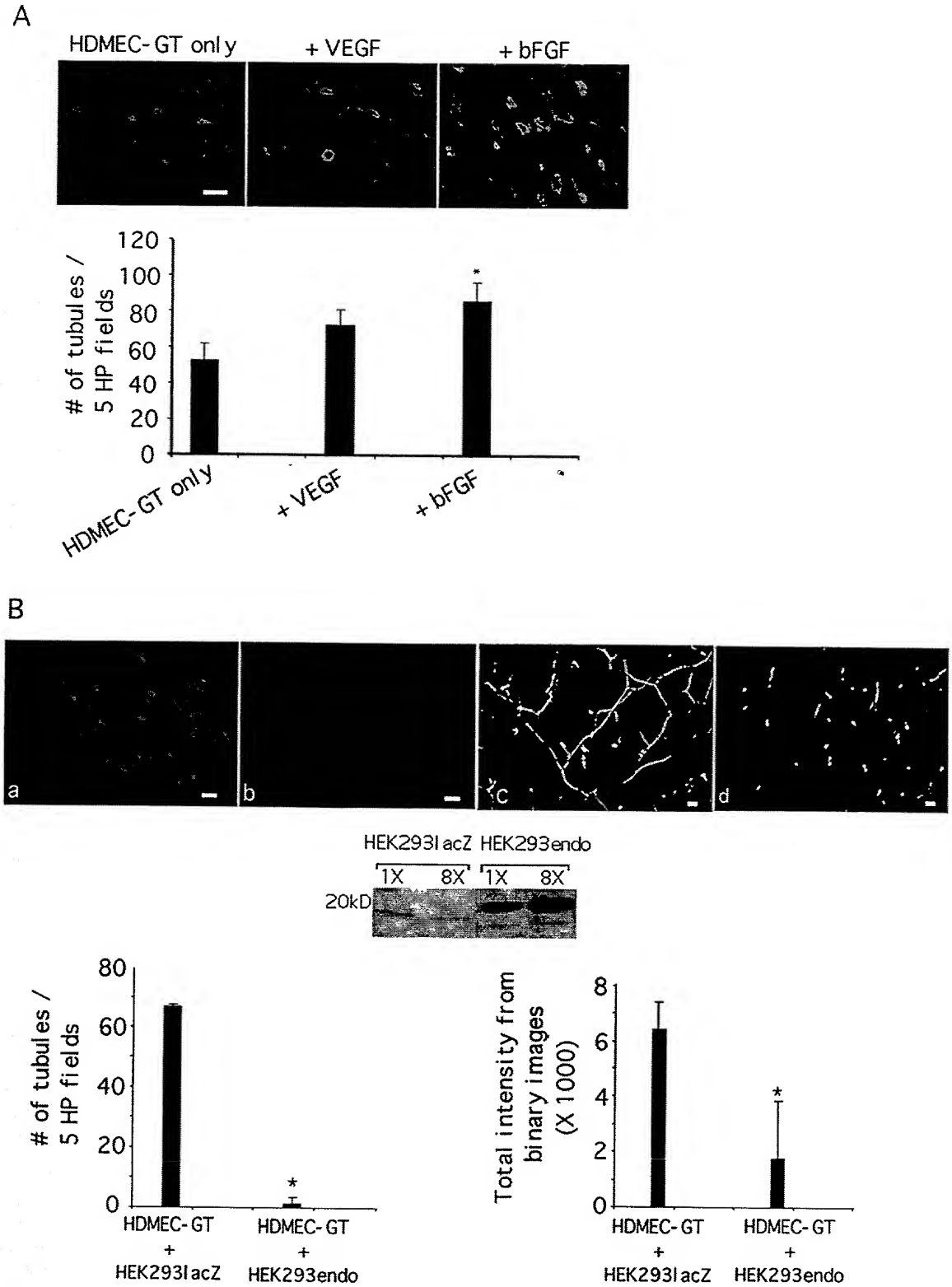
A
HDMEC-GT only
+ VEGF
+ bFGF
# of tubules / 5 HP fields
120
100
80
60
40
20
0
*
HDMEC-GT only
+ VEGF
+ bFGF
B
a
b
c
d
HEK293lacZ
HEK293endo
1X
8X
1X
8X
20kD
# of tubules / 5 HP fields
80
60
40
20
0
*
HDMEC-GT + HEK293lacZ
HDMEC-GT + HEK293endo
Total intensity from binary images (X 1000)
8
6
4
2
0
*
HDMEC-GT + HEK293lacZ
HDMEC-GT + HEK293endo